



Temperature-insensitive refractive index sensor based on in-fiber Michelson interferometer

Zhengyong Li, Yiping Wang*, Changrui Liao, Shen Liu, Jiangtao Zhou, Xiaoyong Zhong, Yingjie Liu, Kaiming Yang, Qiao Wang, Guolu Yin

Key Laboratory of Optoelectronic Devices and Systems of Ministry of Education and Guangdong Province, Shenzhen University, Shenzhen 518060, China



ARTICLE INFO

Article history:

Received 7 February 2014

Received in revised form 11 March 2014

Accepted 16 March 2014

Available online 1 April 2014

Keywords:

Optical fiber sensor

Michelson interferometer

Refractive index

Temperature

ABSTRACT

A novel intensity-modulated refractive index sensor based on an in-fiber Michelson interferometer is demonstrated by splicing a section of thin core fiber between two standard single mode fibers. Such a refractive index sensor exhibits an ultrahigh sensitivity of -208.24 and 125.44 dB/RIU at the refractive index of 1.440 and 1.500, respectively. The refractive index sensor is insensitive to temperature and thus solves the cross-sensitivity problem between temperature and surrounding refractive index. Moreover, the promising RI sensor has the advantages of short size (less than 2 mm) and easy fabrication.

© 2014 Elsevier B.V. All rights reserved.

1. Introduction

In recent years, fiber optic refractive index (RI) sensors in the field of chemical and biomedical applications has attracted significant attentions of researchers due to the advantages of their small size, high sensitivity, short response time, anti electromagnetic interference, and corrosion resistance. One has developed various in-fiber RI sensors based on typical in-fiber devices such as fiber Bragg gratings (FBGs) [1], long period fiber gratings (LPFGs) [2–4], Mach-Zehnder interferometers (MZIs) [5], surface plasmon resonance (SPR) [6], Fabry-Perot interferometers (FPIs) [7,8], Michelson interferometers (MIs) [9–13], and photonic crystal fibers (PCFs) [14]. However, complicated fabrication techniques, such as femtosecond laser micromachining [10], repeated arc discharges [12], fiber taping [13], and chemical etching [9], have employed to achieve refractive index sensors above. For example, a fiber in-line Michelson interferometer tip sensor based on open micro-cavity was fabricated by femtosecond laser micromachining [10]. A miniature core-offset RI sensor was created by means of repeated arc discharges, resulting in melting a fiber end into a rounded tip to excite high order cladding modes [12]. A refractive index sensor based on a Michelson interferometer was demonstrated by tapering abruptly a single mode fiber (SMF) and coating gold on the fiber

end fact [13]. In addition, the wavelength-modulated refractive index sensor usually is sensitive to temperature [9,15,16] so that the cross-sensitivity problem between temperature and surrounding refractive index has to be solved in practical sensing applications [17–20].

In this paper, a novel intensity-modulated refractive index sensor based on in-fiber Michelson interferometer was demonstrated by splicing a section of thin core fiber between two standard SMFs. Such a RI sensor is insensitive to temperature and thus solves the cross-sensitivity problem between temperature and surrounding refractive index. The MI-based RI sensor exhibits an ultrahigh sensitivity of -208.24 and 125.44 dB/RIU at the refractive index of 1.440 and 1.500, respectively.

2. Device fabrication

Microscope image and schematic diagram of our proposed refractive index sensor based on a Michelson interferometer are shown in Fig. 1. One end of a standard SMF (Corning, SMF-28), i.e. SMF1, with a core/cladding diameter of $8.2 \mu\text{m}/125 \mu\text{m}$ was connected to a broadband light source with a wavelength range from 1250 to 1650 nm (Fiber Lake ASE-LIGHT SOURCE) and an optical spectrum analyzer (OSA, YOKOGAWA AQ6370C) with a resolution of 2 nm via a 3 dB coupler in order to observe the reflection spectrum in real time during the fabrication of the MI-based sensor sample. After the right end of SMF1 was cleaved by use of a cutting knife (Fujikura DT-30), the observed reflection spectrum

* Corresponding author. Tel.: +86 13510186456.

E-mail addresses: ypwang@szu.edu.cn, ypwang@china.com (Y. Wang).

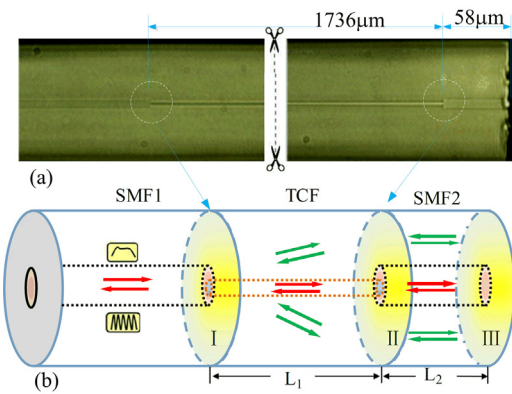


Fig. 1. (a) Microscope image and (b) schematic diagram of the created Michelson interferometer sample. Note that the image is cut off to illustrate the spliced joints of the sample.

was illustrated in Fig. 2(a). Secondly, the cleaved right end of SMF1 was spliced with a thin core fiber (Nufern, UHNA3), i.e. TCF, with a core/cladding diameter of 4 μm/125 μm by use of a commercial fusion splicer (Fujikura FSM-60s). Before and after the right end of the TCF was cleaved, the observed reflection spectra were illustrated in Fig. 2(b) and 2(c), respectively. Interference fringes shown in Fig. 2(c) result from the Fabry–Perot interference between the two end facets of the TCF. Thirdly, another standard SMF (Corning, SMF-28), i.e. SMF2, was spliced with the cleaved right end of the TCF. Before and after the right end of SMF2 was cleaved, the observed reflection spectra were illustrated in Fig. 2(d) and 2(e), respectively. Interference fringes shown in Fig. 2(e) result from the

Michelson interference between the reflected core and cladding modes at the cleaved right end of SMF2, as discussed below.

Since SMF1 has a larger core diameter than the TCF, light propagating through SMF1 will divide into two parts: the core mode with a major energy and the cladding modes with a minor energy, at the interface, i.e. interface-I, between SMF1 and the TCF and then are reflected at the cleaved right end of the TCF. The reflected core and cladding modes will interfere with each other, i.e. Michelson interference, in the core of SMF1. Since the reflected core mode has a much larger energy than the reflected cladding modes, low interference fringe visibility is observed in the reflection spectrum, as shown in Fig. 2(c). In case SMF2 is spliced with the right end of the TCF, the core mode reflected at the cleaved right end facet, i.e. interface-III, of SMF2 will propagate through SMF2 and then transfer partially into the cladding modes at the interface, i.e. interface-II, between the TCF and SMF2, which results in the decrease of the reflected core mode and the increase of the reflected cladding modes in the TCF. Consequently, the reflected core mode has a similar energy to the reflected cladding modes so that high interference fringe visibility was observed in the reflection spectrum, as shown in Fig. 2(e).

As shown in Fig. 1(b), optical distance difference between the reflected core and cladding modes can be given by

$$\Delta d = L_1 \Delta n_{TCF}^m + L_2 \Delta n_{SMF}^m \quad (1)$$

where L_1 and L_2 is the length of the TCF and SMF2, respectively; Δn_{TCF}^m and Δn_{SMF}^m are the effective RI difference between the core mode and the m th order cladding mode in the TCF and SMF2, respectively; so the interference intensity can be calculated by

$$I = I_1 + I_2 + 2\sqrt{I_1 I_2} \cos(\Delta\Phi) \quad (2)$$

where I_1 and I_2 are the intensity of the core and cladding modes, respectively; λ is the wavelength of the propagating light. According to phase matching condition as

$$\Delta\Phi = \frac{4\pi(L_1 \Delta n_{TCF}^m + L_2 \Delta n_{SMF}^m)}{\lambda_m} = (2m + 1)\pi \quad (3)$$

So free spectral range (FSR) in the interference fringe can be calculated by

$$FSR = \frac{\lambda^2}{2(L_1 \Delta n_{TCF}^m + L_2 \Delta n_{SMF}^m)}. \quad (4)$$

As shown in Eq. (4), the FSR depends strongly on the lengths, i.e. L_1 and L_2 , of the TCF and SMF2. So we can achieve a desired FSR by means of improving the length of TCF and SMF2, as described below.

Interference fringe visibility in the reflection spectrum depends strongly on the intensity of the reflected core and cladding modes, which are decided by the lengths of the TCF and SMF2, the core diameters of the TCF and the standard SMF, and the spliced joints. So it is easy for us to enhance interference fringe visibility by means of cleaving gradually SMF2 to improve its length, as shown in Fig. 3, which is a critical advantage of our proposed in-fiber MI structure. In case the lengths of the TCF and SMF2 were improved to be 1736 and 58 μm, respectively, we achieved a desired interference fringe with a high visibility of up to 24 dB. In contrast, the observed fringe visibility of the RI interferometer sensor based on a rounded tip and core-off was only about 5 dB, as reported in ref. [12], in which repeated arc discharges have to done to reshape the fiber end into a rounded tip.

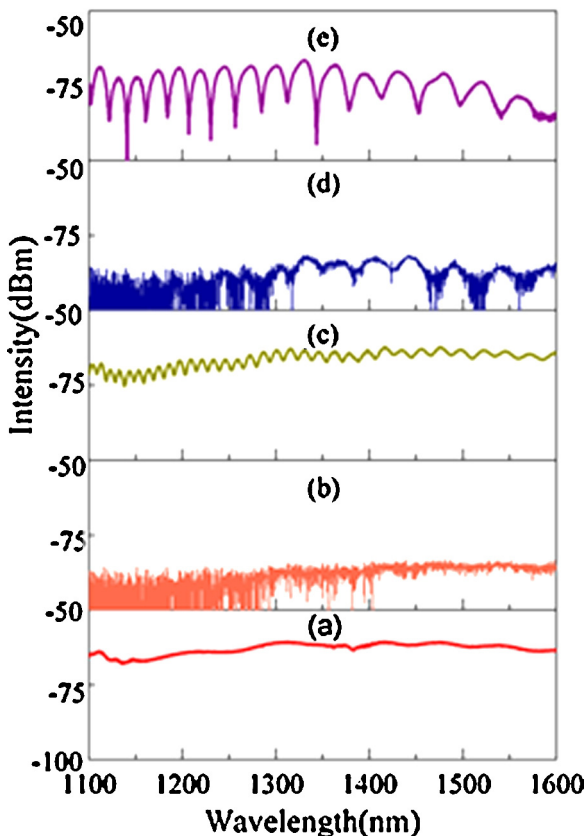


Fig. 2. Reflecion spectra of (a) after the right end of SMF1, (b) before and (c) after the right end of the TCF was cleaved, (d) before and (e) after the right end of SMF2 was cleaved.

3. Index sensing application

We investigated the response of the MI sample to surrounding refractive index by means of immersing it into a series

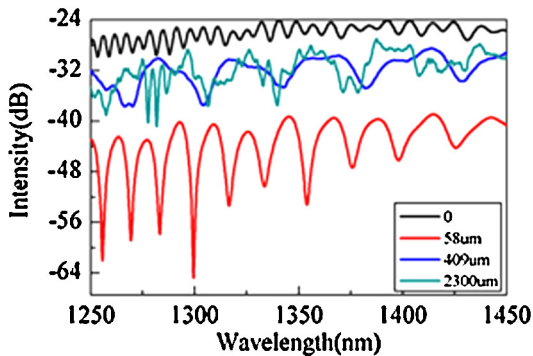


Fig. 3. Reflection spectra of the in-fiber Michelson interferometer while the length of SMF2 is improved to be 0, 58, 409 and 2300 μm . Note that the zero length of SMF2 indicates that no SMF is spliced with the right end of the TCF.

of liquids, e.g. Refractive index matching liquid (Cargille Labs, <http://www.cargille.com>) with a RI from 1.300 to 1.700 at room temperature. Every time the MI sample was taken out from a liquid, it was carefully cleaned by use of alcohol to eliminate entirely the residual liquid on the fiber surface and then was immersed into another liquid.

As shown in Fig. 4(a), the intensity of the reflection spectrum decreased gradually while the surrounding refractive index was changed from 1.000 (air), 1.300 (liquid) to 1.460 (liquid). The reason for this is, that light reflected at the interface-III is gradually reduced with the increased surrounding refractive index, n_{so} from 1.0 to 1.460, according to Fresnel reflection, $R = (n_{\text{si}} - n_{\text{so}})^2 / (n_{\text{si}} + n_{\text{so}})^2$

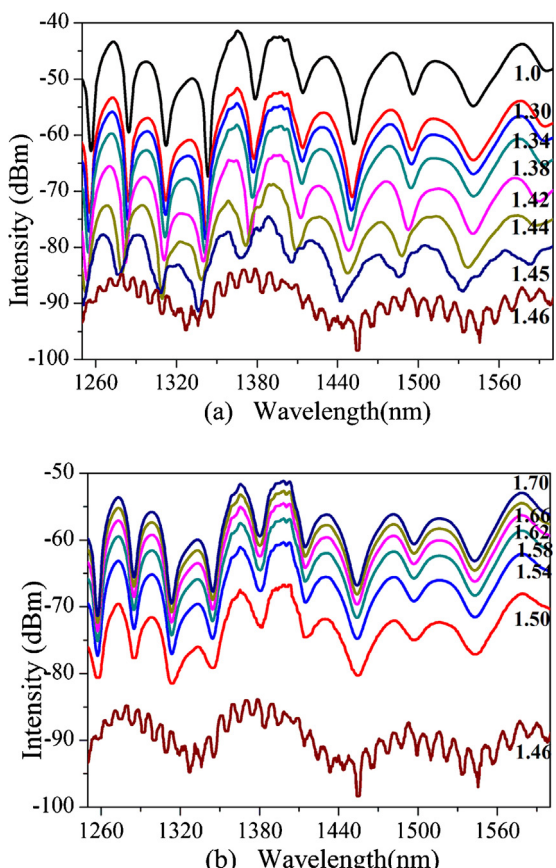


Fig. 4. Reflection spectrum evolution of the in-fiber MI sample immersed into a series of liquid with a refractive index (a) from 1.30 to 1.46, and (b) from 1.46 to 1.70.

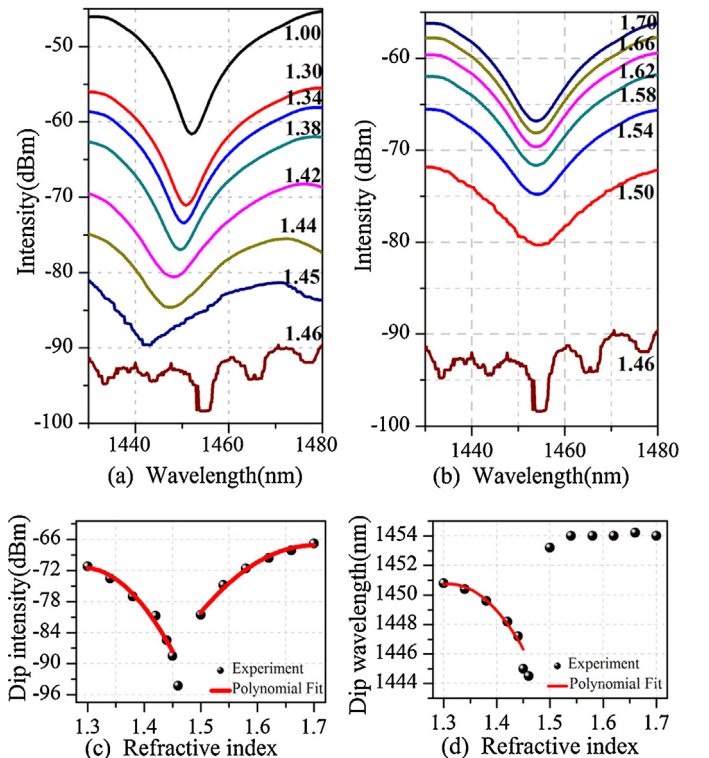


Fig. 5. Reflection spectrum evolution within the wavelength range from 1430 to 1480 nm while the surrounding RI changes (a) from 1.0 to 1.46 and (b) from 1.46 to 1.70; (c) The dip intensity of the interference fringe versus the surround RI; (d) The dip wavelength versus the surrounding RI.

where n_{si} and n_{so} are refractive index of silica and surround medium (air or liquid), respectively. Note that the RI of the fiber material, i.e. silica, is about 1.460. In contrast, as shown in Fig. 4(b), the intensity of the reflection spectrum increased gradually while the surrounding refractive index was changed from 1.460 to 1.700. The reason for this is, according to Fresnel reflection, that light reflected at the interface-III is enhanced gradually with the increased surrounding refractive index, n_{so} , from 1.460 to 1.700. It can be seen from Fig. 4 that, while the MI sample was immersed into a liquid with a similar refractive index (1.460) to silica index, interference fringes with a small FSR of about 10 nm was observed in the reflection spectrum, which results from the Fabry–Perot interference between the interface-II and the interface-III, rather than the Michelson interference, due to the reduce of light reflected at the interface-III.

Reflection spectra within the wavelength range from 1430 to 1480 nm in Fig. 4 are illustrated in Fig. 5(a) and (b) to analyze quantitatively the response of the in-fiber MI sample to the change of surrounding refractive index. As shown in Fig. 5(c), the dip intensity of the interference fringe decreases with the increased surrounding RI from 1.0 to 1.46 and increases with the increased surrounding RI from 1.46 to 1.70. Therefore, such an in-fiber MI could be used to develop a promising intensity-modulated RI sensor. The sensitivity of the MI-based RI sensor is calculated to be -208.24 and 125.44 dB/RIU at the refractive index of 1.440 and 1.500, respectively, via polynomial fitting method.

As shown in Fig. 5(d), the dip wavelength of the interference fringe also decreases with the increased surrounding RI from 1.0 to 1.46, which the wavelength sensitivity of RI sensor is calculated to be -72.87 nm/RIU at the RI of 1.44, and hardly changes with the increased surrounding RI from 1.46 to 1.70, but the intensity modulation, rather than the wavelength modulation, was used in our proposed MI-based refractive index sensor in order to solve the

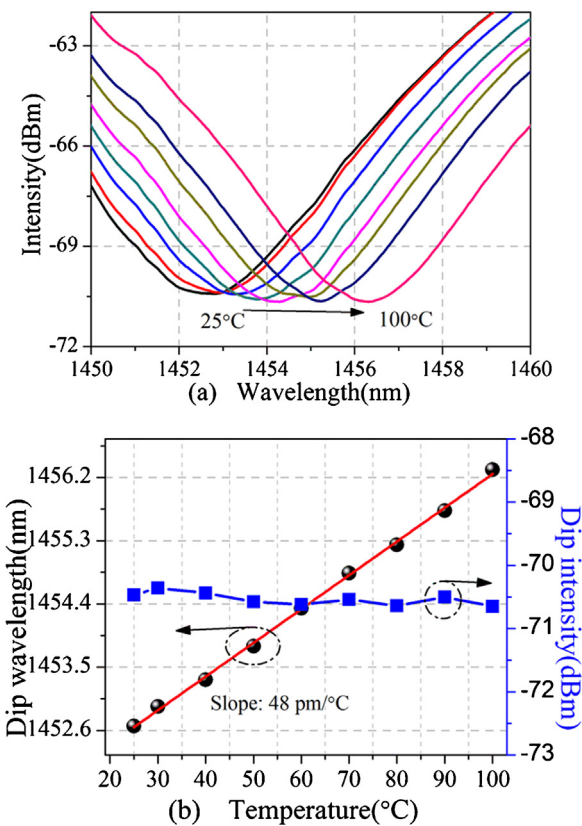


Fig. 6. Reflection spectrum evolution of the in-fiber MI sample (a) temperature rise from 25 to 100 °C with a step of 10 °C.(b) dip wavelength and corresponding dip intensity vary with temperature.

cross-sensitivity problem between temperature and surrounding refractive index, as described below.

4. Temperature response

The cross sensitivity between surrounding refractive index and temperature has to be considered in the application of refractive index sensors. So we investigated the temperature response of the MI-based RI sensor by use of an oven with a temperature stability of ± 0.2 °C. While the temperature rose from room temperature, i.e. 25–100 °C, as shown in Fig. 6(a), the reflection spectrum of the MI-based sensor shifted toward a longer wavelength with a sensitivity of 0.048 nm/°C whereas the dip intensity of the interference fringe hardly changed. In other words, the dip intensity is insensitive to temperature. So our proposed intensity-modulated refractive index sensor based on the in-fiber MI is insensitive to temperature and thus solve the cross-sensitivity problem between temperature and surrounding refractive index.

5. Conclusion

A compact in-fiber MI with a short size of less than 2 mm was created by splicing a section of thin core fiber between two standard SMFs. Interference fringes in the reflection spectrum have a high extinction ratio of up to 24 dB. Such an in-fiber MI could be used to develop a promising intensity-modulated refractive index sensor that exhibits an ultrahigh sensitivity of -208.24 and 125.44 dB/RIU at the refractive index of 1.440 and 1.500, respectively. Moreover, the MI-based refractive index sensor solves the cross-sensitivity problem between temperature and surrounding refractive index

and could find potential applications in the fields of chemical and biomedical sensing, and environmental monitoring.

Acknowledgements

This work was supported by National Natural Science Foundation of China (grant nos. 11174064, 61308027, and 61377090), Science & Technology Innovation Commission of Shenzhen (grant nos. KQCX20120815161444632, and JCYJ20130329140017262), and Distinguished Professors Funding from Shenzhen University (grant nos. 810-000001) and Guangdong Province Pearl River Scholars (grant nos. 829-000001).

References

- [1] X. Fang, C.R. Liao, D.N. Wang, Femtosecond laser fabricated fiber Bragg grating in microfiber for refractive index sensing, *Opt. Lett.* 35 (7) (2010) 1007–1009.
- [2] Y.E. Fan, T. Zhu, L.L. Shi, Y.J. Rao, Highly sensitive refractive index sensor based on two cascaded special long-period fiber gratings with rotary refractive index modulation, *Opt. Lett.* 36 (23) (2011) 4604–4610.
- [3] D.W. Kim, Y. Zhang, K.L. Cooper, A. Wang, In-fiber reflection mode interferometer based on a long-period grating for external refractive-index measurement, *Appl. Opt.* 44 (26) (2005) 5368–5373.
- [4] Y. Fan, T. Zhu, L. Shi, Y. Rao, Highly sensitive refractive index sensor based on two cascaded special long-period fiber gratings with rotary refractive index modulation, *Appl. Opt.* 50 (23) (2011) 4604–4610.
- [5] S.S. Zhang, W. Zhang, P. Geng, S. Gao, Fiber Mach-Zehnder interferometer based on concatenated down- and up-tapers for refractive index sensing applications, *Opt. Commun.* 288 (2013) 47–51.
- [6] P. Bhatia, B.D. Gupta, Surface-plasmon-resonance-based fiber optic refractive index sensor: sensitivity enhancement, *Appl. Opt.* 50 (14) (2011) 2032–2036.
- [7] Y. Wang, D.N. Wang, C.R. Liao, T. Hu, J. Guo, H. Wei, Temperature-insensitive refractive index sensing by use of micro Fabry-Perot cavity based on simplified hollow-core photonic crystal fiber, *Opt. Lett.* 38 (3) (2013) 269–271.
- [8] C.R. Liao, T.Y. Hu, D.N. Wang, Optical fiber Fabry-Perot interferometer cavity fabricated by femtosecond laser micromachining and fusion splicing for refractive index sensing, *Opt. Express* 20 (20) (2012) 22813–22818.
- [9] A. Zhou, G. Li, Y. Zhang, Y. Wang, C. Guan, J. Yang, et al., Asymmetrical twin-core fiber based Michelson interferometer for refractive index sensing, *J. Lightwave Technol.* 29 (19) (2011) 2985–2991.
- [10] C.R. Liao, D.N. Wang, M. Wang, M.H. Yang, Fiber in-line Michelson interferometer tip sensor fabricated by femtosecond laser, *IEEE Photon. Technol. Lett.* 24 (22) (2012) 2060–2063.
- [11] Q. Rong, X. Qiao, Y. Du, D. Feng, R. Wang, Y. Ma, et al., In-fiber quasi-Michelson interferometer with a core-cladding-mode fiber end-face mirror, *Appl. Opt.* 52 (7) (2013) 1441–1447.
- [12] W.C. Wong, C.C. Chan, Y.F. Zhang, K.C. Leong, Miniature single-mode fiber refractive index interferometer sensor based on high order cladding mode and core-offset, *IEEE Photon. Technol. Lett.* 24 (5) (2012) 359–361.
- [13] Z.B. Tian, S.S.H. Yam, H.P. Looch, Refractive index sensor based on an abrupt taper Michelson interferometer in a single-mode fiber, *Opt. Lett.* 33 (10) (2008) 1105–1107.
- [14] D.Q. Yang, H.P. Tian, Y.F. Ji, Q.M. Quan, Design of simultaneous high-Q and high-sensitivity photonic crystal refractive index sensors, *J. Opt. Soc. Am. B: Opt. Phys.* 30 (8) (2013) 2027–2031.
- [15] Y. Wang, D. Richardson, G. Brambilla, X. Feng, M. Petrovich, M. Ding, et al., Intensity measurement bend sensors based on periodically tapered soft glass fibers, *Opt. Lett.* 36 (4) (2011) 558–560.
- [16] Y. Wang, D.N. Wang, W. Jin, CO₂ laser-grooved long period fiber grating temperature sensor system based on intensity modulation, *Appl. Opt.* 45 (31) (2006) 7966–7970.
- [17] Y. Wang, L. Xiao, D.N. Wang, W. Jin, Highly sensitive long-period fiber-grating strain sensor with low temperature sensitivity, *Opt. Lett.* 31 (23) (2006) 3414–3416.
- [18] Y.J. Rao, X.K. Zeng, Y. Zhu, Y.P. Wang, T. Zhu, Z.L. Ran, et al., Temperature-strain discrimination sensor using a WDM chirped in-fibre Bragg grating and an extrinsic Fabry-Perot, *Chin. Phys. Lett.* 18 (5) (2001) 643–645.
- [19] J. Grochowski, M. Mysliwiec, P. Mikulic, W.J. Bock, M. Smietana, Temperature cross-sensitivity for highly refractive index sensitive nanocoated long-period gratings, *Acta Phys. Polon. A* 124 (3) (2013) 421–424.
- [20] K.M. Zhou, L. Zhang, X.F. Chen, I. Bennion, Optic sensors of high refractive-index responsivity and low thermal cross sensitivity that use fiber Bragg gratings of >80 degrees tilted structures, *Opt. Lett.* 31 (9) (2006) 1193–1195.

Biographies

Zhengyong Li was born in Hubei Province, China in 1988. He received his bachelor degree from Huazhong University of Science and Technology Wenhua College in 2012. He is currently completing his master degree in the field of fiber optic sensors in Shenzhen University, China.

Yiping Wang is a Distinguished Professor and a Pearl River Scholar in the College of Optoelectronic Engineering, Shenzhen University, Shenzhen, China. He was born in Chongqing, China, in July 15, 1971. He received the B.S. degree in Precision Instrument Engineering from Xi'an Institute of Technology, Xi'an, China, in 1995, and the M.S. degree in Precision Instrument and Mechanism and the Ph.D. degree in Optical Engineering from Chongqing University, China, in 2000 and 2003, respectively, where he received the prestigious award of The National Excellent Doctoral Dissertations of China. In 2003, he joined the Department of Electronics Engineering, Shanghai Jiao Tong University, China, as a postdoctoral research fellow and an associate professor. In 2005, he joined the Department of Electrical Engineering, Hong Kong Polytechnic University, Hong Kong, as a postdoctoral research fellow and a research fellow. In 2007, he joined the Institute of Photonic Technology, Jena, Germany as a Humboldt research fellow. In 2009, he joined the Optoelectronics Research Centre, University of Southampton, U.K. as a Marie Curie Fellow. Since 2012, he has been with Shenzhen University as a Distinguished Professor and a Pearl River Scholar. His current research interests focus on optical fiber sensors, in-fiber gratings, photonic crystal fibers, and fluid-filling technologies. He has authored or coauthored 1 book, 9 patent applications, and more than 150 journal and conference papers with a SCI citation of more than 1200 times. Dr. Wang is a senior member of IEEE, the Optical Society of America, and the Chinese Optical Society.

Changrui Liao received the B.E. degree in optical information science and technology and the M.S. degree in physical electronics from Huazhong University of Science and Technology, China, in 2005 and 2007, and the Ph.D. degree from the Hong Kong Polytechnic University, Hong Kong, in 2012. Since 2012, he has been with the College of Optoelectronic Engineering, Shenzhen University as an assistant professor. His main research interests are femtosecond laser micromachining, optical fiber devices and sensors.

Shen Liu was born in Henan Province in China in 1986. He was awarded his master degree in Chongqing University of Posts and Telecommunications.

Jiangtao Zhou was born in Anhui province in China in 1990. He is currently completing his master degree in the field of fiber optic sensors in Shenzhen University, China.

Xiaoyong Zhong was born in Guangdong Province in China in 1988. He received bachelor degree in Guangdong University of Technology. He is currently completing his master degree in the field of fiber optic sensors in Shenzhen University, China.

Yingjie Liu was born in Hubei Province, China in 1989. She is currently completing her master degree in the field of fiber optic sensors in Shenzhen University, China.

Kaiming Yang was born in Jiangxi Province in China in 1991. He is currently completing his master degree in the field of fiber optic sensors in Shenzhen University, China.

Qiao Wang was born in Hubei Province, China in 1991. He received his bachelor from Huazhong university of science and technology wenhua college in 2013. He is currently completing his master degree in the field of fiber optic sensors in Shenzhen University, China.

Guolu Yin received bachelor degree and Ph.D. from Department of Science in Beijing Jiaotong University in 2008 and in 2013, respectively. He joined in Shenzhen University, China, as a postdoctoral fellow.